Synthesis of Kit-of-parts Structures for Reuse

Jan Brütting[1,*], Gennaro Senatore[2], Alex Muresan[1], Ioannis Mirtsopoulos[1], Corentin Fivet[1]

[1] Structural Xploration Lab, Swiss Federal Institute of Technology Lausanne (EPFL), 1700 Fribourg, Switzerland

[*] Corresponding author e-mail: jan.bruetting@epfl.ch

[2] Applied Computing and Mechanics Laboratory, Swiss Federal Institute of Technology Lausanne (EPFL), 1015 Lausanne, Switzerland

Abstract

This paper shows a computational workflow to design a kit of parts consisting of linear bars and spherical joints that can be employed to assemble, take apart, and rebuild diverse reticular structures, e.g. gridshells and space frames. Being able to reuse bars and joints among different structures designed with this method reduces the material demand compared to one-off construction. The input of the method is a set of different reticular structures intended to be built from a common kit of parts. In a first step, the structure geometries are optimised such that the structures share groups of members with identical lengths to allow the placement of same bars in all structures. In a second step, the kit-of-parts joints are optimised to allow their reuse in different structures as well. This is achieved by merging the specific connection patterns of nodes from different structures into one joint. The potential of the proposed method is demonstrated via its application to two case studies: 1) the design of three temporary space frame roofs, and 2) the realisation of three pavilion-scale prototypes serving as a proof of concept. The latter case study also shows the robotic fabrication of the bespoke joints.

Keywords: kit of parts, structures, reuse, form finding, clustering, space frames, joints, robotic fabrication

1 Introduction

1.1 Motivation

Recent trends in architectural and structural design build on the potential of *reuse* to reduce the environmental footprint of building structures (Iacovidou and Purnell 2016; Gorgolewski 2017). For instance, it has been shown that reusing reclaimed structural elements from obsolete buildings for a second life time avoids raw material use, requires few energy, and reduces waste (Fivet and Brütting 2020; Brütting et al. 2020). An alternative approach consists in synthesizing a *kit of parts* from new materials such that its components are reusable in diverse structural configurations. In other words, multiple structures successively use a common stock of components, which reduces material demand compared to one-off constructions. Although applicable to any building system (Howe et al. 1999; Brancart et al. 2017), the strategy is particularly relevant when designing temporary support structures for different uses and sites, e.g. for exhibitions and events.

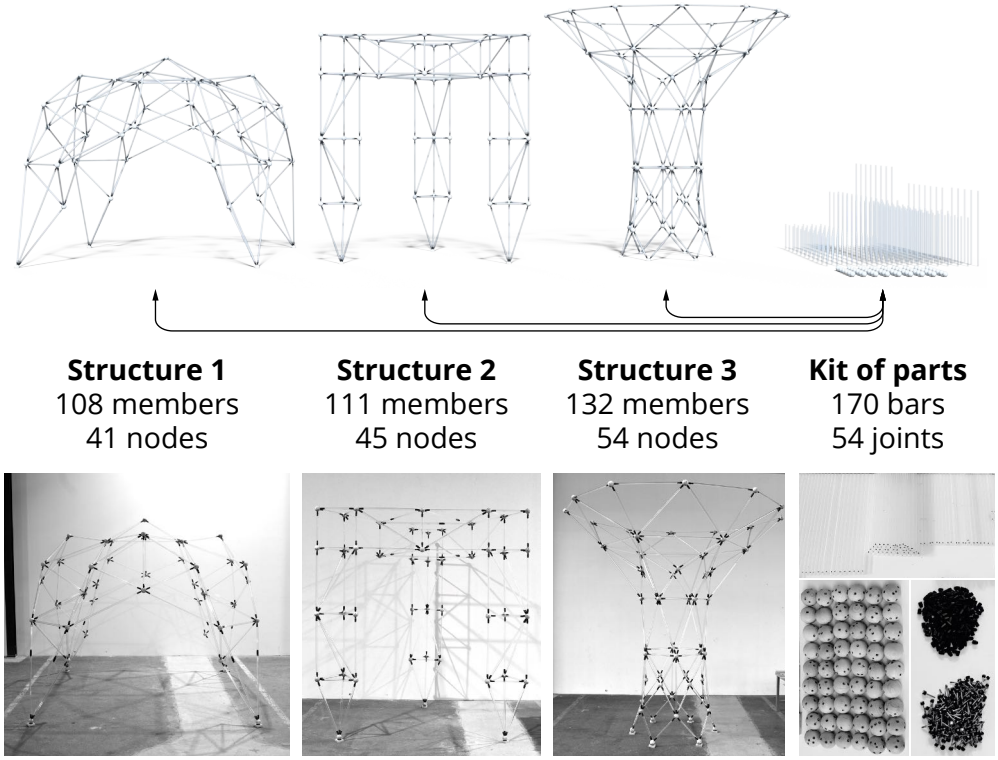

Figure 1: Kit of parts to build three pavilion-scale structures. Because bars and joints are reused among structures, the kit of parts consists of less components than the three structures have in total.

This paper shows a computational workflow to design a kit of parts whose linear bars and spherical joints can be used to build a set of diverse structures, e.g. trusses, gridshells, and space frames. Different to existing solutions, the structure geometries produced by this method are not restricted to repetitive modular arrangements (**fig. 1**). All connections between parts are reversible to allow for multiple (re-) assemblies.

1.2 Related work

Making complex architectural free-form surfaces and support structures (e.g. roofs or facades) affordable in monetary terms and feasible for manufacturing has been the focus of many architectural geometry *rationalisation* methods (Austern et al. 2018). The main driver of these methods is the cost reduction through batch production of identical elements. Following the same motivation, Lobel (1993) showed rules to design a large number of polyhedral surfaces that consist of identical equilateral triangles only. Similarly, Jiang et al. (2015) and Huard et al. (2014) presented the panellisation of free-form surfaces with identical equilateral triangles and Fu et al. (2010) as well as Singh and Schaefer (2010) showed the tiling of surfaces with clusters of quads and triangles. Placing structural members along the edges of panels obtained with these methods gives clusters of members with identical lengths.

An under-explored potential of these sophisticated rationalisation methods is that one could apply them to multiple surfaces or structures simultaneously in order to obtain architectural designs where identical elements could be shared among different systems, making possible the reuse of elements. Zimmer et al. (2014) presented a method to approximate different free-form shapes with a kit of parts ("Zometool systems"). However, this system is limited to bars of nine different lengths and universal nodes with 62 prescribed connection directions.

Typically, modular construction systems are employed when designing and building temporary structures for multiple service cycles. The MERO space frame system composed of tubular linear bars and universal nodal joints is probably the most prominent example. One drawback of the system however is its restriction to certain module geometries such as tetrahedra and octahedra (Mengeringhausen 1975). Following recent advances in architectural geometry modelling and manufacturing, sophisticated construction systems have been developed for more complex free-form reticular structures (Schober 2015; Hassani et al. 2020). However, most parts in these structures remain bespoke to a defined location. Even though it was never the customary objective of these systems, such customisation hinders the potential to reuse parts among structures.

In contrast with existing solutions, the method shown in this paper considers the simultaneous design of multiple structures as well as the manufacturing of linear bars and nodal joints such that all parts can be reused in different non-modular structures.

2 Method

In the following the term *member* refers to the link between two nodes in a structure. The kit-of-parts *bars* and *joints* are the physical entities that are placed at member and node positions during structure assembly. In general, designing a common kit of parts for multiple structures implies that all parts have to geometrically fit to positions in different structures and all connections must be reversible to allow multiple assemblies (Brancart et al. 2017). This section shows the two main steps of the method: 1) the simultaneous form finding of a finite set of structure geometries such that members of identical lengths exist in all structures, and 2) the optimisation of the joints to make them fit to nodes in different structures.

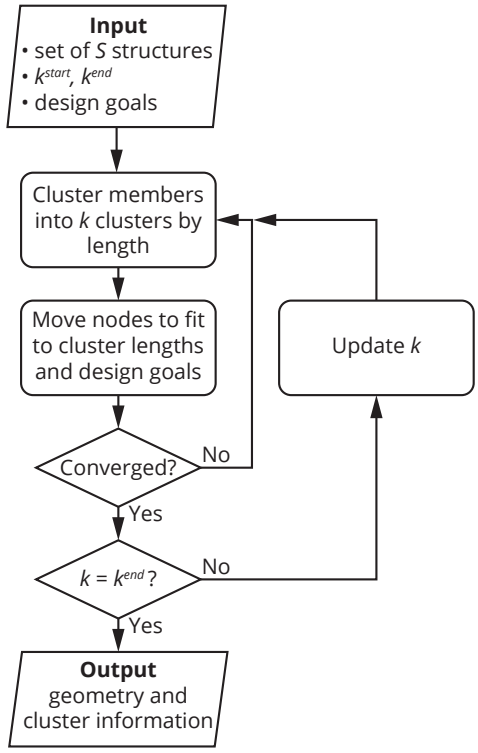

Figure 2: Flow chart of the form finding and member length clustering method.

2.1 Form finding

The form finding process is summarised by the flow chart shown in **fig. 2**. Inputs are the layouts (geometry and topology) of the $s = 1 \dots S$ structures that are foreseen to be built from the kit of parts. First, all $i = 1 \dots m_{tot}$ members of all S structures are clustered into a defined starting number of k^{start} groups based on their member lengths l_i. For the clustering, a univariate *k-means* algorithm (Wang and Song 2011) that is particularly suited for 1-dimensional data (lengths) is employed. The mean length of all members within a cluster c is denoted cluster length l_c, where $c = 1 \dots k$. Next, the node positions of all structures are optimised with the objective to match the member lengths with the length l_c of the cluster to which the members have been assigned through k-means. In this work, a customised implementation of the software *Kangaroo Physics v. 2.42* (K2) (Piker 2020) is employed for the optimisation of node positions: for each member a *length goal* (Piker 2016) with the 'rest-length' being l_c is defined. Member length clustering and optimisation of structure node positions are iteratively repeated until convergence (close matching of member and cluster lengths). If needed, the number k of clusters is then incrementally increased or decreased until it equals a given k^{end} (**fig. 2**). k^{end} determines the eventual number of different bar lengths in the kit of parts.

Figure 3 illustrates the form finding method for two reticular structures with 12 and 11 members, respectively. Member lengths are clustered into $k = 3$ groups (**fig. 3b**). The structure geometries obtained after convergence of the form finding process (**fig. 3c**) display members with identical lengths in each cluster (**fig. 3d**). Members of same length can be shared and reused among both structures. Therefore, the kit of parts must contain only as many bars as maximally used in one of the two structures (grey regions in **fig. 3d**). The number of bars per cluster and length is denoted n_c. In order to be able to consecutively build the two structures, $n_{tot} =$ 15 bars are necessary in total. The quality of a form finding solution is measured through the *homogenisation rate* HR, which is defined as HR $= m_{tot}/n_{tot}$, where m_{tot} is the total number of members in all structures. For the example in **fig. 3**, HR $= 23/15 = 1.53$. In general, the aim is to obtain a large HR value, meaning that many bars are reused.

Throughout the form finding process, depending on the input structure layouts and selected value for k, it might not always be possible to exactly match member and cluster lengths. When this is the case, bars must be manufactured with the length of the shortest member in the cluster, resulting in a length difference (or gap) Δ between members and bars. In practice, such gap could be filled with custom spacers of specific thicknesses (e.g. 1 mm, 2 mm, ...).

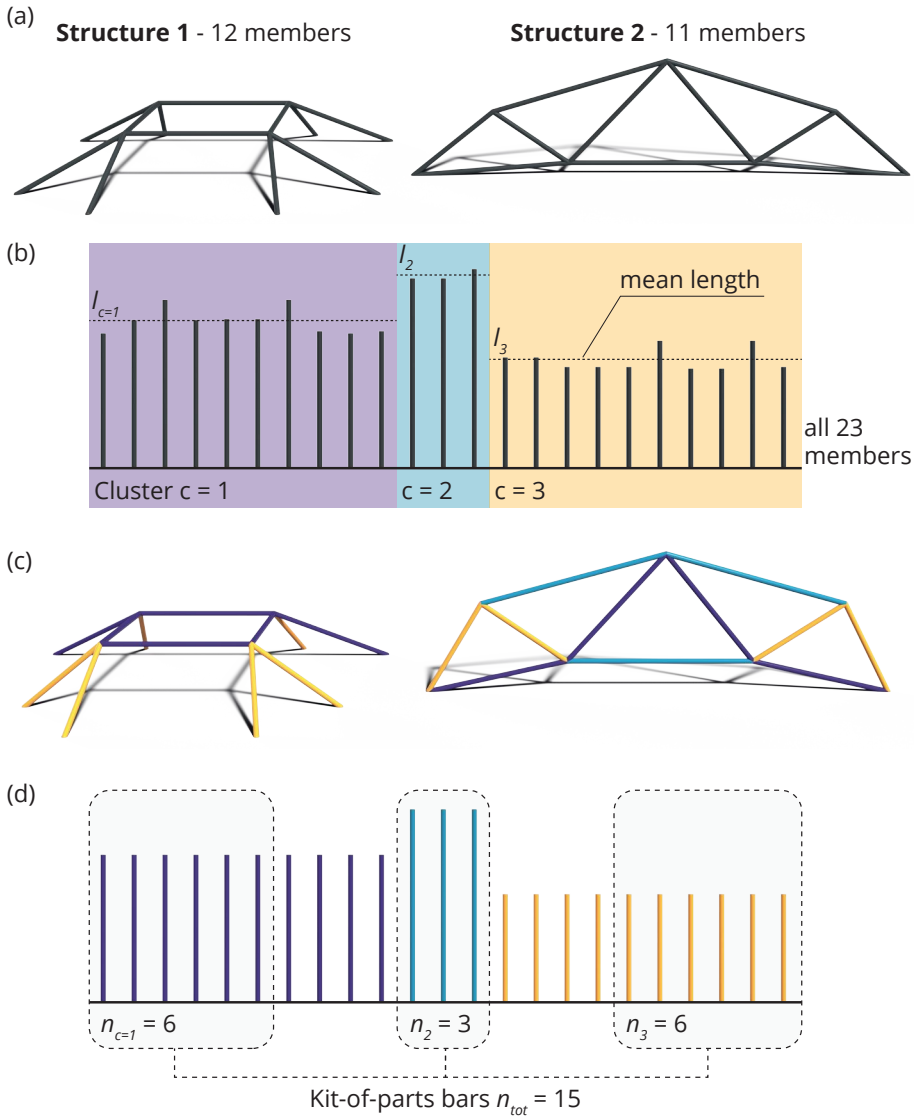

Figure 3: Example of the form finding method: (**a**) input structures, (**b**) member length clustering into $k = 3$ groups, (**c**) form-found geometries, and (**d**) selection of the subsets of members that make up the kit of parts. Cluster colours in (**b**) and members colours in (**c**) and (**d**) correspond.

The advantage of employing K2 as form finding engine is its potential for combining the clustering of member lengths with many other design *goals* (objectives and constraints), either those that are available in the K2 library (Piker 2020) or custom scripted ones (Piker 2016). For example, a minimum angle to be respected between adjacent members can be prescribed to avoid interference of bars. In K2, goals are combined using weighting factors w and inputs can be parametrically adapted which allows for a user interactive design.

2.2 Joint optimisation

This work considers reticular structures in which bars are connected at nodes via spherical joints, fastened together with bolts (see also **fig. 6**, **sec. 3.2**). The bolts are screwed into holes located on the joint sphere surface. This section presents an optimisation method to design joints that fit given node positions in different structures, which allows the reuse of joints among structures.

Figure 4a gives an example of three nodes that are merged into one bespoke joint. The hole sets that have to be combined in one joint are shown by the red, white, and blue cylinders at the top of **fig. 4a**. The directions of holes in a set is defined by the directions of the members pointing to the respective node. Placement of holes on the joint is optimised in order to distribute holes evenly over the joint spherical surface. The aim is to avoid locally concentrated perforations and by doing so to increase the mechanical capacity of the joints. In addition, partial overlapping of holes must be avoided. In the optimisation, the hole sets are rotated about the joint sphere centre as complete entities (**fig. 4b**) applying the following unconstrained optimisation problem:

$$\min_{\boldsymbol{\varphi}} \left(-\frac{1}{R^3} V(\boldsymbol{\varphi}) + \sum_h p(\alpha_h(\boldsymbol{\varphi})) \right) \tag{1}$$

In **eq. (1)**, the vector $\boldsymbol{\varphi}$ holds the rotations of the hole sets about the X-, Y- and Z-axis (**fig. 4b**). The first term in the objective function maximises the volume $V(\boldsymbol{\varphi})$ of the *convex hull* (**fig. 4c**) which is computed from the centres of all holes. In general, the larger the volume of the convex hull the better the holes are distributed. The factor $1/R^3$, with R being the joint sphere radius, unitises the volume function. The second term in the objective function is a penalty function meant to avoid partial overlapping of holes. The penalty term p is computed for every central angle $\alpha_h(\boldsymbol{\varphi})$ between a pair h of adjacent holes (**fig. 4c**). The penalty value varies according to a sinusoidal from 0 when adjacent holes are either superimposed or clearly separated, to 1 when they are in an in-between state:

$$p(\alpha_h(\boldsymbol{\varphi})) = \begin{cases} 0 & \text{if } \alpha_h(\boldsymbol{\varphi}) \geq \alpha_{min} \\ \sin\left(\frac{\alpha_h(\boldsymbol{\varphi})}{\alpha_{min}}\pi\right) & \text{if } 0 \leq \alpha_h(\boldsymbol{\varphi}) \leq \alpha_{min} \end{cases} \tag{2}$$

The minimum angle α_{min} that must be respected between two adjacent holes is computed from the joint radius R, the hole depth D, and the hole width W (**fig. 4b**):

$$\alpha_{min} = 2 \cdot \tan^{-1}\left(\frac{W/2}{R-D}\right) \tag{3}$$

For a fixed hole depth D and width W, the larger the sphere radius R, the easier it is to avoid collisions of holes. The optimisation problem (**eq. (1)**) is highly non-linear and non-convex and the computation of a convex hull is non-differentiable. The genetic algorithm of Matlab (The Math Works Inc. 2018) is therefore employed as a solver in this work.

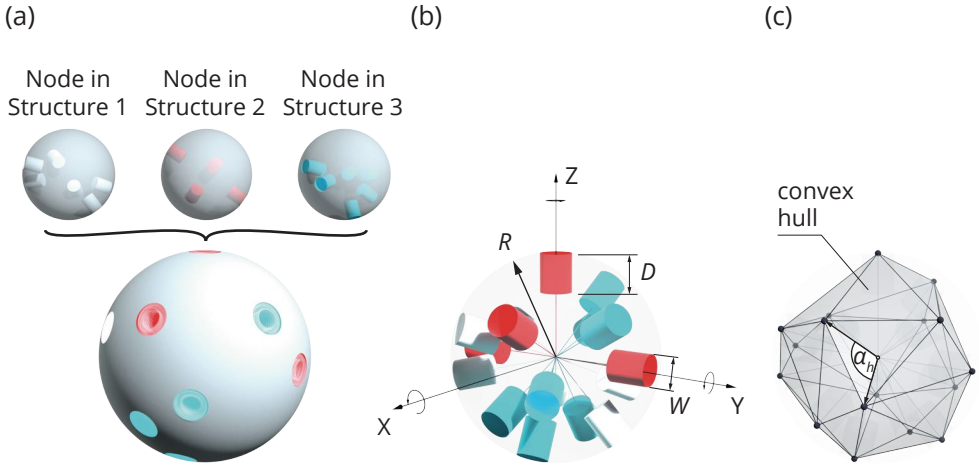

Figure 4: Joint optimisation to reuse joints among structures: (**a**) merging of nodes from different structures into one joint, (**b**) rotation of hole sets about the joint central axes, and (**c**) convex hull computed from the hole centres.

3 Case studies

3.1 Complex space frames

This section shows the application of the method to design a kit of parts for three space frame structures with complex geometry. These structures are thought of as support structures for roofs consecutively installed for temporary events (**fig. 5a**). Structure 1 is an array of arches over a passage, Structure 2 is an undulating and elongated roof above a stairway, and Structure 3 is a square roof over a courtyard. Covering of the space frames with panels is out of scope of this study.

Form finding results

Figure 5a shows the input structure layouts considered for the form finding. Only the double-layered space frame parts of the structures and not the support columns that are present in Structures 2 and 3 are part of the form finding. The number of bays in each structure (subdivision) has been manually selected such that all members have lengths between 2.00 and 4.60 metres. The three structures contain 420, 320, and 392 members respectively ($m_{tot} = 1132$). The red dots in **fig. 5a**

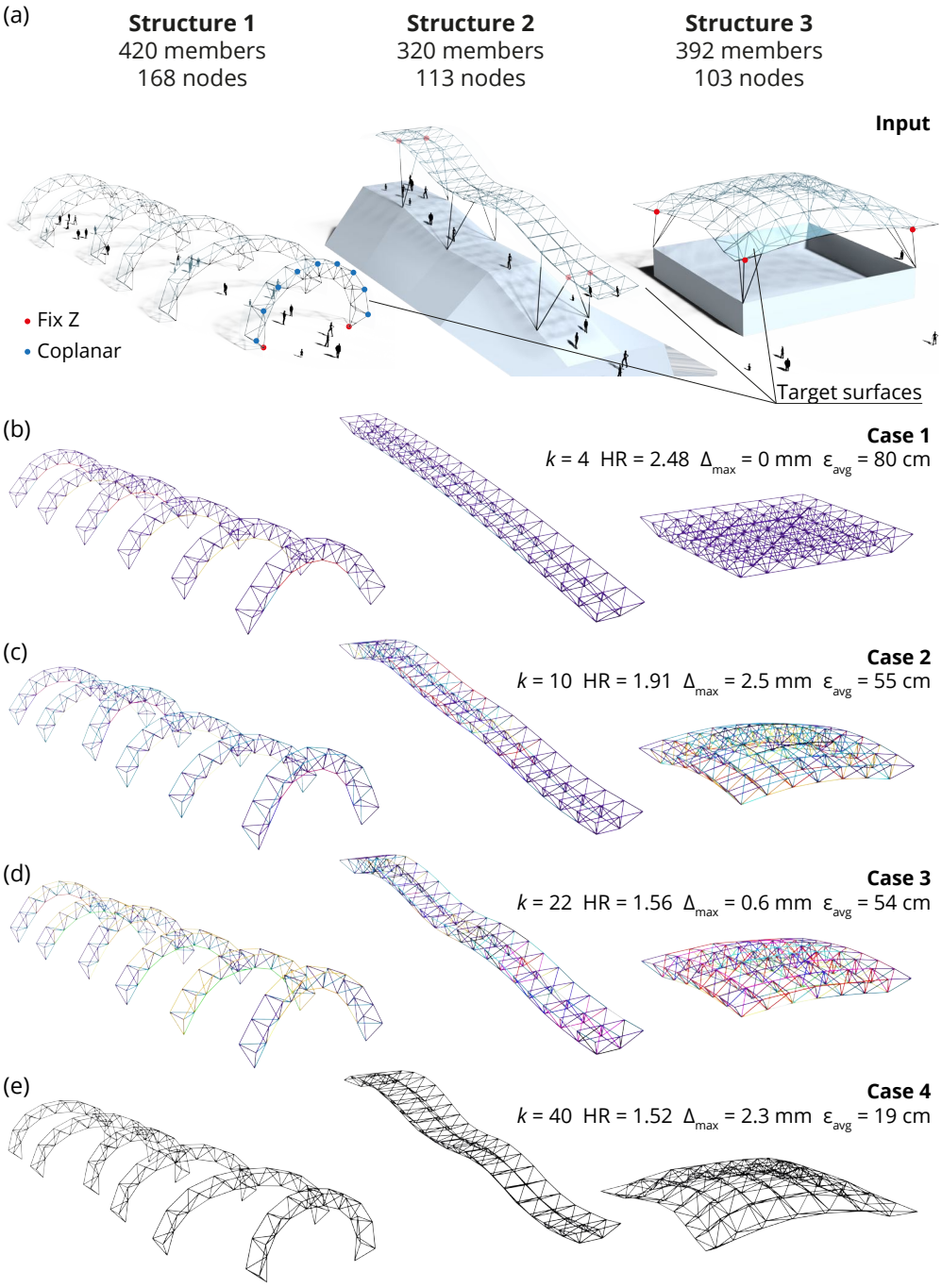

Figure 5: Form finding results: (**a**) input layouts and (**b**-**e**) results for cases 1) to 4) with variation in the number of clusters k; in (**b**-**d**) members of same colour belong to the same length cluster; colour mapping in (**e**) is omitted due to the large value of k.

show the nodes for which the Z-coordinate has been fixed in the form finding. Next to the member length clustering, two additional design goals are considered in this study: proximity of the structure top layer nodes to the target surfaces, and co-planarity of the nodes located at each edge of the arches in Structure 1 (**fig. 5a**, blue dots). The weighting factors for the length goal (**sec. 2.1**), surface proximity, and co-planarity are denoted by w_L, w_P, and w_C, respectively. In general, w_L is chosen orders of magnitude larger than w_P and w_C because matching of member and cluster lengths is a hard constraint to be able to reuse bars. The maximum gap between member and cluster lengths is denoted Δ_{max}. The average distance of the top layer nodes to their respective target surfaces is denoted ε_{avg}.

In this section, four cases with variation in the number of clusters ($k^{end} = 4$, 10, 22, and 40) as well as in the weighting factors w_L, w_P, and w_C are studied. **Figure 5b-e** shows the form-found geometries and **tab. 1** summarises obtained results for all considered cases. As shown by **fig. 5b-e**, employing a small number of clusters generally gives structure geometries that are further off from the target shapes. A greater k allows more variation in bar lengths, which in turn gives a better proximity of the kit-of-parts solution to the target shape (ε_{avg}).

For case 1) with $k^{end} = 4$ clusters, the structure geometries are quite regular. For example, Structure 3 only contains members of identical length (purple bars in **fig. 5b**) and for Structures 2 and 3 the curved appearance of the input is lost. However, this regularity reduces the total number of kit-of-parts bars required to $n_{tot} = 456$ (HR = 2.48, **tab. 1**) and all members within a cluster have identical lengths ($\Delta_{max} = 0$).

Case	k^{start}	k^{end}	w_L	w_P	w_C	#bars n_{tot}	HR	Δmax	n|Δ = 0-0.49 mm	n|Δ = 0.5-1.49 mm	n|Δ = 1.5-2.49 mm	n|Δ ≥ 2.5 mm	ε_{avg}	CPU time
	[-]	[-]	$\cdot 10^3$	[-]	[-]	[-]	[-]	[mm]	[-]	[-]	[-]	[-]	[cm]	[s]
1	1	4	10	2	5	456	2.48	0	1132	0	0	0	80	9
2	1	10	10	2	5	594	1.91	2.5	195	453	481	3	55	22
3	1	22	50	2	10	727	1.56	0.6	1099	33	0	0	54	51
4	20	40	80	2	10	744	1.52	2.3	487	604	41	0	19	42

Table 1: Form finding results.

A higher number of clusters ($k^{end} = 10$) in case 2) gives a smaller homogenisation rate of HR = 1.91 and a maximum gap of $\Delta_{max} = 2.5$ mm between bar and member lengths. **Table 1** shows the distribution of gap sizes in steps of 0.5 mm. Actually, the gap is 2.5 mm for only three member positions and the majority of gaps is smaller than 1.5 mm. In practice, these numbers refer to the amount of custom spacers that must be placed between bars and joints if such small length differences are not negligible.

In cases 3) with $k^{end} = 22$ clusters, the curved shapes of the input structures are preserved better. Yet, this comes with a further reduction in homogenisation rate to HR $= 1.56$. The weighting factor w_L is increased to $5 \cdot 10^4$ to obtain a small length gap ($\Delta_{max} = 0.6$ mm). Case 4) has a high number of 40 clusters and serves as a benchmark: to remain close to the input geometry in total 744 bars are required (HR $= 1.52$).

The rightmost column in **tab. 1** shows that the computation times for the form finding (obtained on an Intel i7-6820HQ CPU) are small and that an interactive design process for kit-of-parts structures is possible.

Joint optimisation results

The three structures have 168, 113, and 103 nodes respectively (384 in total). **Table 2** gives metrics for the initial case where joints are manufactured for a single node, and for two optimisation cases J1) and J2) following the method shown in **sec. 2.2**. J1) decreases the number of joints while J2) decreases the total volume of the joints. In the initial case, the joint sphere radius can be small ($R = 29$ mm)

Case	Joint Radius R	# joints n_{tot}	homog. rate HR	total volume V_{tot}
	[mm]	[-]	[-]	[dm^3]
initial	29	384	1.00	39.2 (100%)
J1	37	168	2.29	35.6 (91%)
J2	33	186	2.06	28.0 (71%)

Table 2: Joint optimisation results.

because less holes need to fit onto a joint sphere surface. Instead, if multiple selected nodes of different structures are merged into one common joint, a larger joint sphere radius is required. As shown by case J1) in **tab. 2**, spheres must have a radius of $R = 37$ mm to obtain the minimum number of joints (168, i.e. the number of nodes in Structure 1). All of the 168 joints are unique and combine nodes of up to three structures. The total volume V_{tot} of 168 joints with $R =$ 37 mm is 35.6 dm^3, which is 91% of the individual solution with 384 smaller joints (39.2 dm^3). In case J2), only nodes with medium nodal valence are merged in order to avoid difficult distributions of holes. For some nodes with high valence and complex hole sets instead an individual joint is considered. This way in total more joints than in case J1) are required (186) but a smaller radius ($R = 33$ mm) is possible. The homogenisation rate for joints in case J2) is lower but the total volume is reduced to 28.0 dm^3 which is 71% of the initial case.

The results show that material input can be reduced through merging of nodes into reusable joints. In practice, the selection of joint sphere radii might also be

constrained by available standard sizes (e.g. $R = 30$, 35, 40 mm etc.). The average computation time to optimise one joint (cases J1 and J2) has been 11 seconds.

3.2 Pavilion-scale proof of concept

This section shows the application of the proposed method to the design of three pavilion-scale prototypes (**fig. 1**, **sec. 1**). This case study serves as a proof of concept for the proposed design and fabrication workflow.

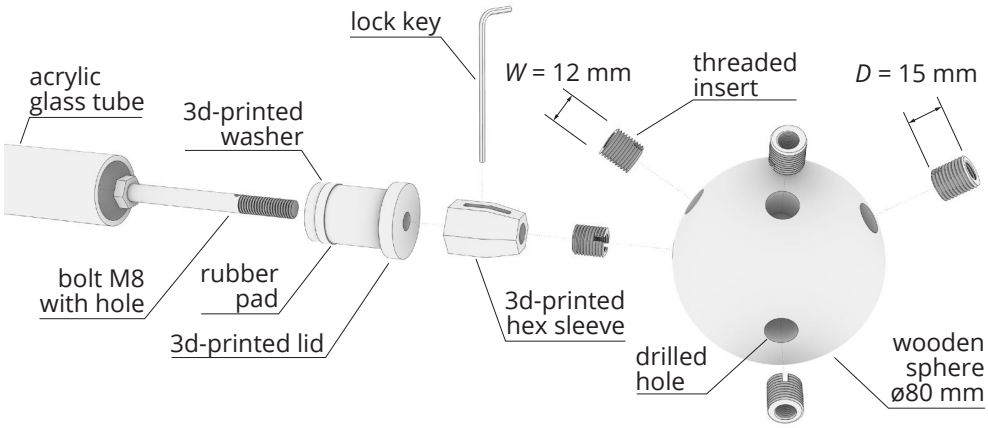

Figure 6: Connection detail of the pavilion prototype.

Detailing

Figure 6 shows the joint design and connector parts used to fasten joints to bars via bolts. The design is inspired by the MERO system but adapted for fabrication with available tools. Acrylic glass tubes are used as bars and wooden spheres are used as joints to obtain a lightweight, transportable system. Based on the joint optimisation results, holes are drilled into wooden spheres and threaded inserts are employed to receive the bolts. The bolt is fastened from the outside via a lock key because the bolt head is not accessible. Transfer of compression forces between joints and bars is achieved through surface contact between all parts. Resistance in tension between inner tube wall and lid is provided by friction as a rubber pad laterally expands when the bolt is tightened. This way the designed connection is fully reversible, thus permitting multiple re-assemblies. For the pavilion application, where small loads are expected, the mechanical capacity of the connection has been sufficient. Different materials such as steel and welded or screwed connections between tubes and intermediate parts should be considered for larger scale.

Form finding and manufacturing of bars

The three input structure geometries are shown at the top of **fig. 7**. The form finding provided best results with $k^{start} = 9$ and $k^{end} = 6$. A computation time ranging between 2.0 to 7.0 seconds allows for the manual adaptation of input layouts as well as interactive addition of design constraints. For instance, upward pointing vertical 'loads' are applied to Structure 1 in order to steer the geometry towards an inverted hanging model. **Figure 7b** shows the resulting structure geometries that were deemed satisfactory from an aesthetic, reuse, and fabrication point of view ($\Delta_{max} \leq 0.1$ mm). The six different bar lengths are 432, 732, 829, 989, 1126, and 1479 mm. Only $n_{tot} = 170$ bars are required to build the three structures with a total of 351 members (HR = 2.06, **fig. 1**).

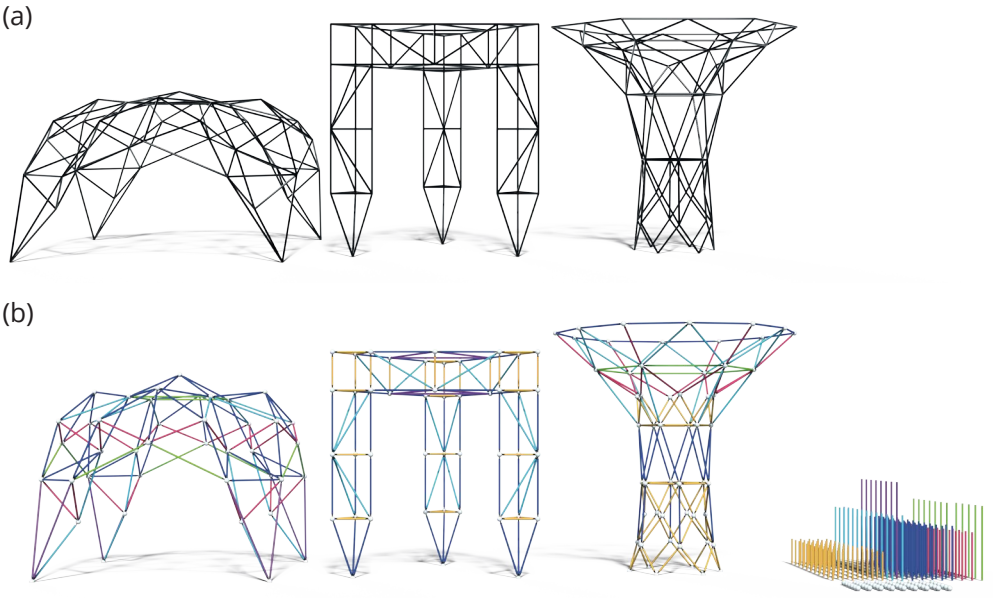

Figure 7: Pavilion case study: (**a**) input structure layouts, and (**b**) form found geometries and kit of parts. In (**b**), structure members and kit of parts bars of same colour have identical length.

For the realisation of the pavilion structures, the tube cross-sections are preliminarily sized based on an adapted version of the optimisation method shown in (Brütting et al. 2019). A conventional finite element analysis is then employed to verify the cross-section sizing and the global stability of the structures. The so obtained cross-section sizes of the bars are ø20/16, ø25/21, and ø30/26 mm (outer / inner diameter), where bars of larger section are placed at member positions with high demand. Those sizes are also selected to allow the sliding of bars into each other in order to reduce the packaging volume for transport.

Joint optimisation and fabrication

The three structures have 41, 45, and 54 nodes respectively. In order to reduce the number of joints to manufacture, it is decided to merge nodes into the minimum number of joints possible (54), which results in joints with 40 mm radius. If one joint would have been manufactured for each of the 140 nodes individually, a smaller joint sphere radius of $R = 37.5$ mm could have been used. However, 54 joints with 40 mm radius have only 47% of the material volume of 140 joints with 37.5 mm radius.

After optimal hole directions are obtained via the joint optimisation method, joints are manufactured following the steps shown in **fig. 8**. First, a 'master hole' is manually drilled into each joint sphere (**fig. 8a**). Then, a threaded insert (**fig. 6**) is screwed into the master hole to allow the mounting of the joint onto the flange of an industrial robotic arm (**fig. 8b**). Further, the master hole also determines the orientation of the joint sphere in space. Next, the bespoke hole patterns are drilled into the joints by manoeuvring the joint onto a stationary drill with the robotic arm (**fig. 8c**).

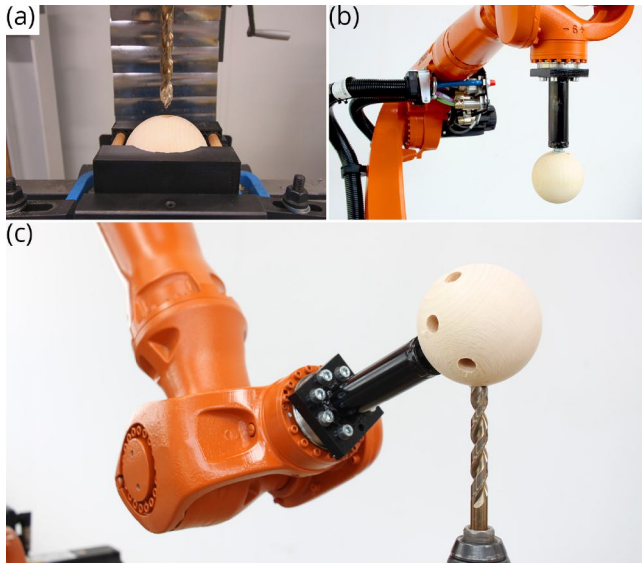

Figure 8: Joint manufacturing: (**a**) Drilling of first 'master hole', (**b**) mounting of joint sphere on robot arm via master hole, and (**c**) drilling of spatial hole pattern via robotic arm and stationary drill.

Kit of parts and assembly

The kit of parts contains 170 bars of six different lengths and 54 spherical joints. **Figure 9** illustrates some of the manufactured and 3d-printed parts as well as the entire kit of parts. The unused holes that can be seen on the surface of the assembled joint shown in **fig. 10** are used in one of the other structure configurations.

The small black dots next the holes are encoding the information to which structure a joint hole belongs. Figure 11 shows the prototype structures consecutively assembled, taken apart, and reassembled.

Figure 9: All components of the kit of parts.

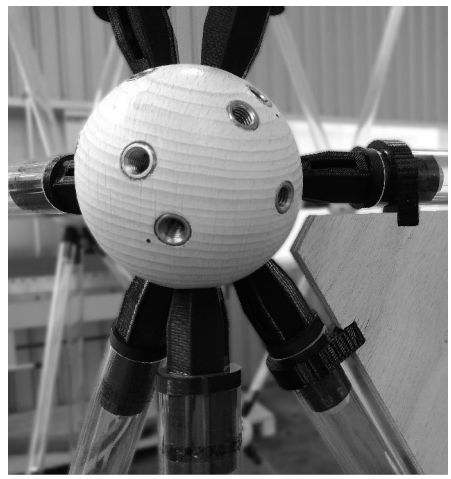

Figure 10: Detailed view of a spherical joint.

4 Discussion and future work

From a structural point of view, spherical joints work best in double layer, triangulated structures where they are primarily subjected to axial forces. In single layer structures, depending on the loading and structure geometry, the members, joints, and centric bolts might be subjected to bending moments. Future work could extend the idea of merging multiple nodes into one joint to other joint types such as bending resistant ones. The hole pattern optimisation has been successfully carried out with the use of a genetic algorithm, yet relatively long computation times are required. Future work could study different ways of formulating the joint optimisation problem or employ different solving techniques other than meta-heuristics.

The focus of this paper was the form finding of structure geometries in order to reuse bars among structures. In general, designing a kit of parts whose components are reused among structures requires considering all load cases that the components experience over all uses (Brütting et al. 2019). Future work could study in more detail the simultaneous member clustering and structural geometry optimisation. In this work, a *k-means* algorithm has been employed for member clustering. This method is simple and easy to integrate into the form finding process. However, it requires as input the number of clusters k. Future work could study different clustering methods and machine learning techniques to improve the member clustering, of special interest would be those methods where the optimal number of clusters is an output.

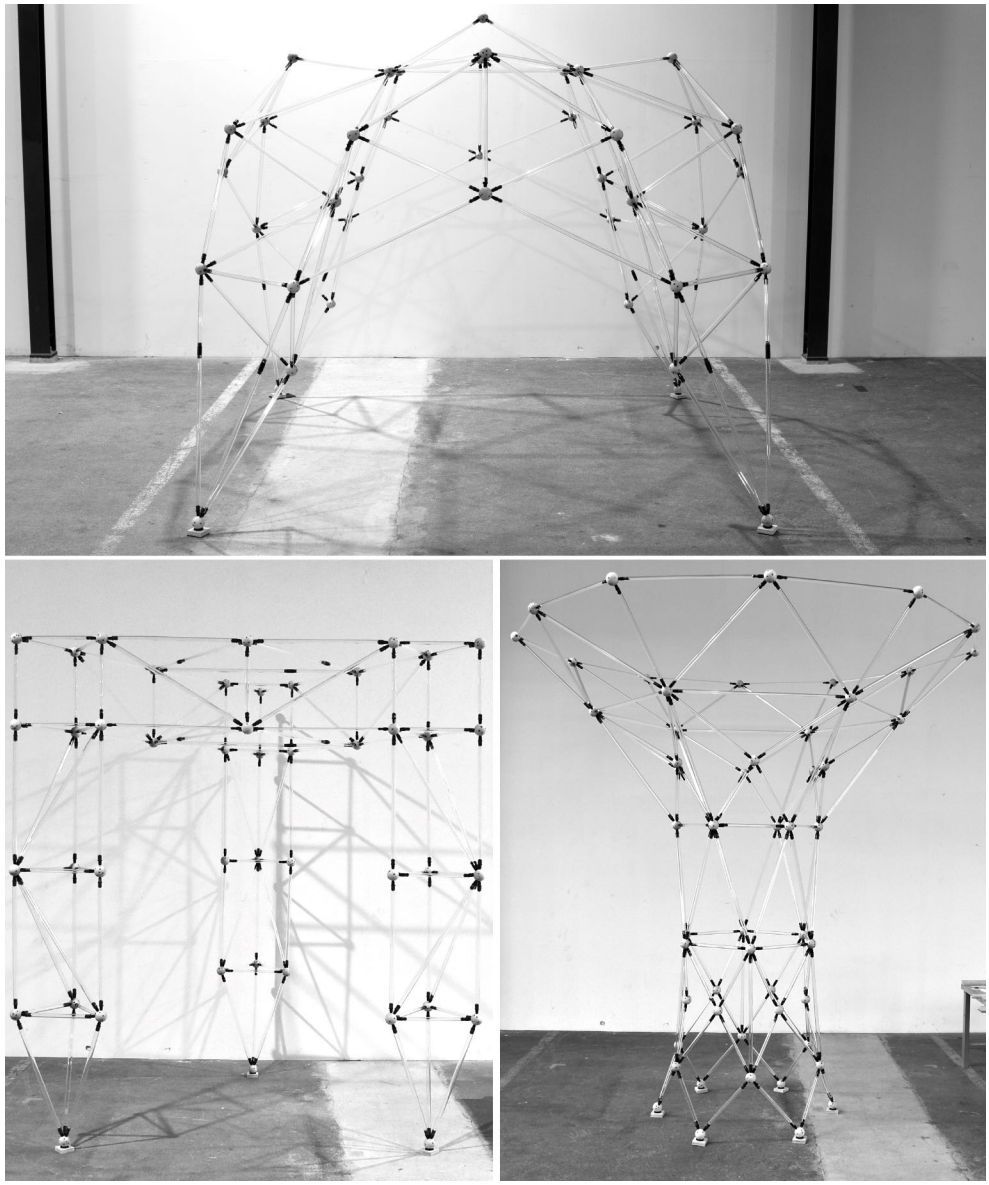

Figure 11: Detailed view of the three assembled pavilion structures.

In practice, structures require cover panels when used as roofs. Panelling has been out of scope of this work but could be combined with member length clustering in future work in order to allow the reuse of bars and joints as well as panels among structures.

5 Conclusion

This paper shows the design and fabrication of a kit of parts consisting of linear bars and spherical joints to build disparate non-modular structures. The structures themselves are meant to serve different uses and to be built at different locations. Bars and joints are designed such that they geometrically fit to positions in different structures and hence they can be reused for multiple service cycles. The proposed form finding method to design kit-of-parts bars and structure geometries allows for user interaction, fast computations, and customisation. In addition, a new method to optimise the connection pattern of spherical joints allows to design joints that can be reused at nodes of different structures whilst considering manufacturing constraints. Manufacturing only a subset of elements to build multiple structures might also reduce monetary costs for material input and fabrication compared to one-off construction.

A proof of concept of the proposed design method has been shown through the realisation of three pavilion-scale structures, including the robotic manufacturing of bespoke joints. A diverse set of structures has been realised with already established fabrication methods. These prototype structures highlight the potential to extend the method to existing space frame systems and to large-scale practical applications. In summary, this paper exhibits how the reuse of parts among different structures opens new research directions for architectural geometry design and rationalisation.

Acknowledgements

The authors would like to thank Claude-Alain Jacot, Prateek Kumar, and Cornelius Carl for their dedicated help throughout manufacturing, assembly, exhibition, and documentation of the prototype pavilions. Financial support from Smart Living Lab, KUKA Switzerland, Debrunner, and Opitec for prototyping and manufacturing is thankfully acknowledged.

References

Austern, G., I. G. Capeluto, and Y. J. Grobman (2018). Rationalization methods in computer aided fabrication: A critical review. *Automation in Construction 90*, 281–293.

Brancart, S., A. Paduart, A. Vergauwen, C. Vandervaeren, L. De Laet, and N. De Temmerman (2017). Transformable structures: Materialising design for change. *International Journal of Design & Nature and Ecodynamics 12*(3), 357–366.

Brütting, J., G. Senatore, and C. Fivet (2019). Form follows availability - Designing structures through reuse. *Journal of the International Association for Shell and Spatial Structures 60*(4), 257–265.

Brütting, J., C. Vandervaeren, G. Senatore, N. De Temmerman, and C. Fivet (2020). Environmental impact minimization of reticular structures made of reused and new elements through Life Cycle Assessment and Mixed-Integer Linear Programming. *Energy and Buildings 215*, 109827.

Fivet, C. and J. Brütting (2020). Nothing is lost, nothing is created, everything is reused: structural design for a circular economy. *The Structural Engineer 98*(1), 74–81.

Fu, C.-W., C.-F. Lai, Y. He, and D. Cohen-Or (2010). K-set tilable surfaces. *ACM Trans. Graph. 29*(4), 1–6.

Gorgolewski, M. (2017). *Resource Salvation: The Architecture of Reuse*. Hoboke, NJ, USA: John Wiley & Sons.

Hassani, V., Z. Khabazi, H. A. Mehrabi, C. Gregg, and R. W. O'Brien (2020). Rationalization algorithm for a topologically-optimized multi-branch node for manufacturing by metal printing. *Journal of Building Engineering 29*, 101146.

Howe, A. S., I. Ishii, and T. Yoshida (1999). Kit-of-parts - A review of object-oriented construction techniques. In *Proceedings of the ISARC'99 - International Symposium on Automation and Robotics in Construction*, Madrid, pp. 165–171.

Huard, M., M. Eigensatz, and P. Bompas (2014). Planar Panelization with Extreme Repetition. In P. Block, J. Knippers, N. J. Mitra, and W. Wang (Eds.), *Advances in Architectural Geometry 2014*, Cham, pp. 259–279. Springer International Publishing.

Iacovidou, E. and P. Purnell (2016). Mining the physical infrastructure: Opportunities, barriers and interventions in promoting structural components reuse. *Science of The Total Environment 557-558*, 791–807.

Jiang, C., C. Tang, M. Tomi**v**cí, J. Wallner, and H. Pottmann (2015). Interactive Modeling of Architectural Freeform Structures: Combining Geometry with Fabrication and Statics. In P. Block, J. Knippers, N. J. Mitra, and W. Wang (Eds.), *Advances in Architectural Geometry 2014*, Cham, pp. 95–108. Springer International Publishing.

Lobel, A. (1993). *Formes et structures engendrées par des éléments identiques*. Bourg-la-Reine: A. Lobel.

Mengeringhausen, M. (1975). *Raumfachwerke aus Stäben und Knoten: Theorie, Planung, Ausführung* (7 ed.). Wiesbaden: Bauverlag.

Piker, D. (2016). Dan-Piker/K2Goals. `https://github.com/Dan-Piker/K2Goals` (Accessed 2020-08-18).

Piker, D. (2020). Kangaroo3d. `http://kangaroo3d.com/` (Accessed 2020-08-18).

Schober, H. (2015). *Transparent Shells: Form, Topology, Structure* (1 ed.). Berlin, Germany: Ernst & Sohn.

Singh, M. and S. Schaefer (2010). Triangle surfaces with discrete equivalence classes. In *ACM SIGGRAPH 2010 papers*, SIGGRAPH '10, Los Angeles, California, pp. 1–7. Association for Computing Machinery.

The Math Works Inc. (2018). Matlab R2018a.

Wang, H. and M. Song (2011). Ckmeans.1d.dp: Optimal k-means Clustering in One Dimension by Dynamic Programming. *The R journal 3*(2), 29–33.

Zimmer, H., F. Lafarge, P. Alliez, and L. Kobbelt (2014). Zometool shape approximation. *Graphical Models 76*(5), 390–401.